

## Supplementary Materials

### Engineered rare-earth nanomaterials for fluorescence imaging and therapy

Hongru Wang <sup>1,2</sup>, Zheng Wei <sup>3</sup>, Yangyang Zhao <sup>5</sup>, Shidong Wang <sup>4,\*</sup>, Lili Cao <sup>2,\*</sup>, Fan Wang <sup>3</sup>, Kai Liu <sup>3,5</sup> and Yanfei Sun <sup>3,\*</sup>

<sup>1</sup>Department of Neurology, Liaocheng People's Hospital, Liaocheng, Shandong, 252000, China

<sup>2</sup>Department of Neurology, Qilu Hospital of Shandong University, Jinan, Shandong, 250012, China

<sup>3</sup>State Key Laboratory of Rare Earth Resource Utilization, Changchun Institute of Applied Chemistry, Chinese Academy of Sciences, Changchun 130022, China

<sup>4</sup>Musculoskeletal Tumor Center, Peking University People's Hospital, Beijing, 100044, China

<sup>5</sup>Department of Chemistry, Tsinghua University, Beijing 100084, China

\*Correspondence: stonewang@bjmu.edu.cn; qiluccl@163.com; Sunyf90@163.com

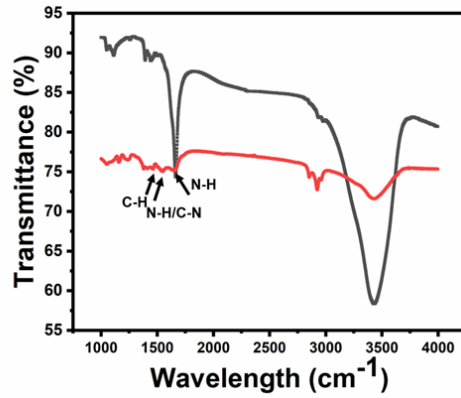


**Fig. S1.** The Fourier Transform Infrared (FTIR) spectroscopy of pristine UCNP (no oleate ligands capped, black) and UCNP@Au (red) nanoparticles. The successful coating of PEI on UCNP is confirmed by the FTIR spectrum with a peak at 1502  $\text{cm}^{-1}$ .

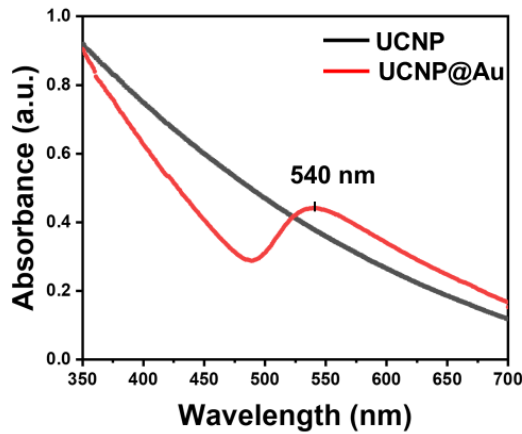


**Fig. S2.** Ultraviolet–Visible (UV-Vis) spectra of UCNP@PEI and UCNP@Au aqueous solution. The UV-Vis spectra of UCNP@Au nanoparticles showed a strong absorption at 540 nm, resulting from the plasma resonance absorption peak of isotropic Au nanoparticles.

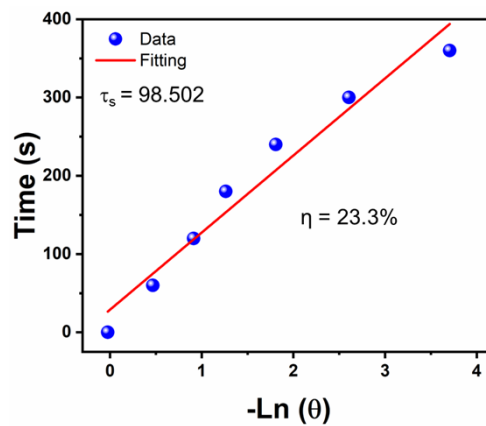


**Fig. S3.** The photo-thermal conversion efficiency ( $\eta$ ) of UCNP@Au.  $\eta$  was calculated as follows [1]:  
 $\eta = hS(T_{\text{max,NPs}} - T_{\text{max,solvent}}) / I(1 - 10^{-A_{980}})$ ;  $t = -\tau_s \text{Ln}\theta$ ;  $\theta = (T - T_{\text{surr}}) / (T_{\text{max,NPs}} - T_{\text{surr}})$ ;  $hS = m_d C_d / \tau_s$ .  $m_d = 1 \text{ g}$ ,  $C_d = 4.2 \text{ J} \cdot \text{g}^{-1} \cdot \text{C}^{-1}$ ,  $T_{\text{max,NPs}} = 49.4 \text{ }^\circ\text{C}$ ,  $T_{\text{max,solvent}} = 30.8 \text{ }^\circ\text{C}$ ,  $T_{\text{surr}} = 25 \text{ }^\circ\text{C}$ ,  $A_{980} = 0.625$ ,  $I = 4.458 \text{ W} \cdot \text{cm}^{-2}$ .

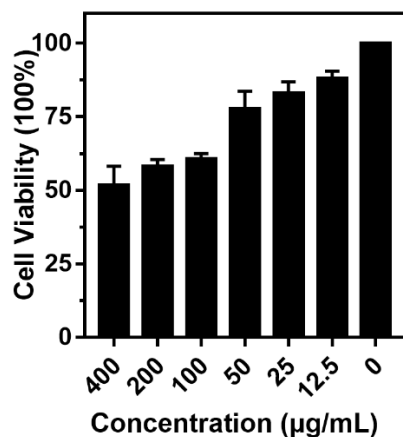


**Fig. S4.** Cell counting kit-8 (CCK8) assay for the cytotoxicity of UCNPs@Au nanoparticles in mouse embryonic fibroblast cell lines (NIH-3T3) cells.

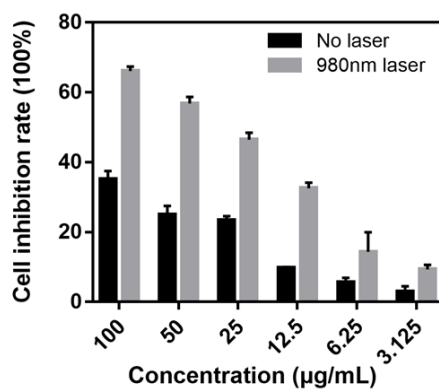


**Fig. S5.** CCK-8 assay to measure the anti-tumour effect of UCNPs@Au nanoparticles in mouse glioma 261 (GL261) cells. Different concentrations of UCNPs@Au nanoparticles were used under the 980 nm laser.

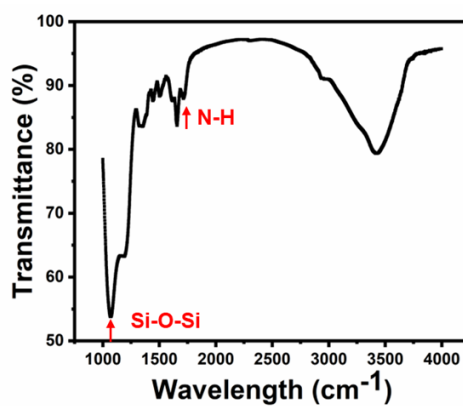


**Fig. S6.** The FTIR spectrum of the UCNPs@mSiO<sub>2</sub>@TA-Al nanoparticle. The formation of the Si–O–Si framework is evidenced by the band located at 1080 cm<sup>-1</sup>. The band located at 1650 cm<sup>-1</sup>, which corresponds to the bending vibration –NH– group indicates the presence of amino groups in

UCNPs@mSiO<sub>2</sub>-NH<sub>2</sub>.

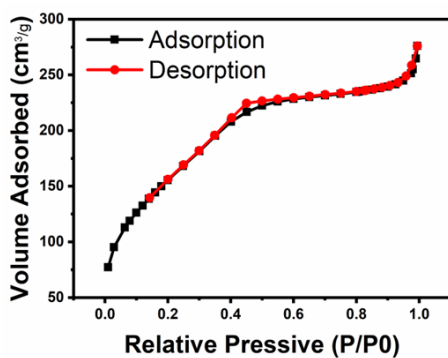


Fig. S7. Nitrogen adsorption-desorption isotherms for UCNPs@mSiO<sub>2</sub>.

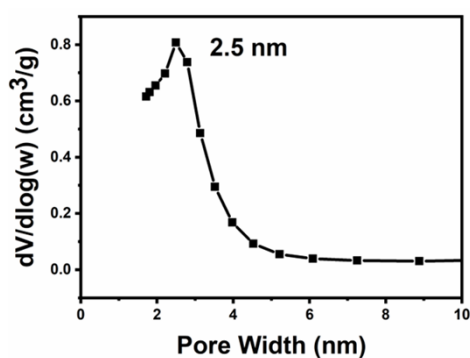


Fig. S8. Pore size analysis for UCNPs@mSiO<sub>2</sub>.

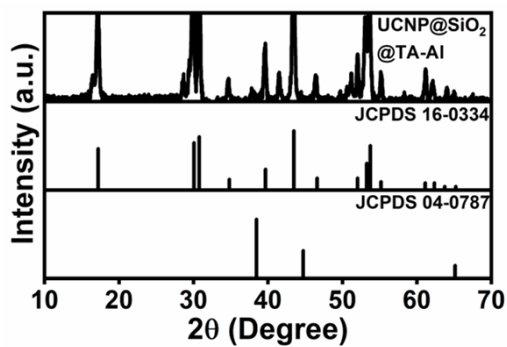
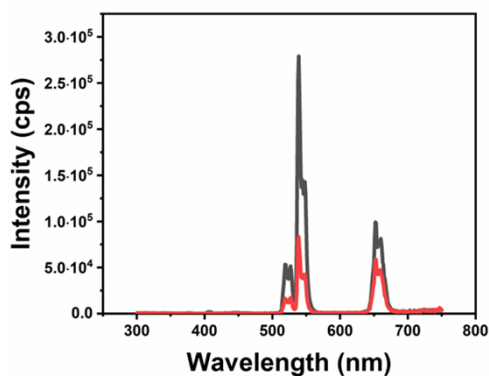
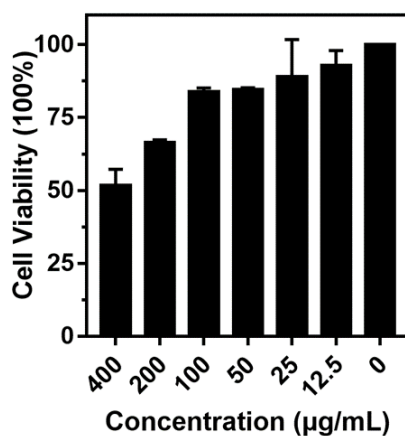


Fig. S9. Powder X-ray Diffraction (XRD) spectra of the UCNPs@mSiO<sub>2</sub>@TA-Al nanoparticle. Standard card of β-NaYF<sub>4</sub> (JCPDS no. 16-0334) and Al (JCPDS 04-0787) were presented.



**Fig. S10.** Upconversion fluorescence emission spectra of UCNPs@mSiO<sub>2</sub> (black) and UCNPs@mSiO<sub>2</sub>@TA-Al nanoparticle (red). They were excited with a 980 nm NIR laser.



**Fig. S11.** CCK-8 assay to examine the cytotoxicity of UCNPs@mSiO<sub>2</sub>@TA-Al in NIH-3T3 cells.

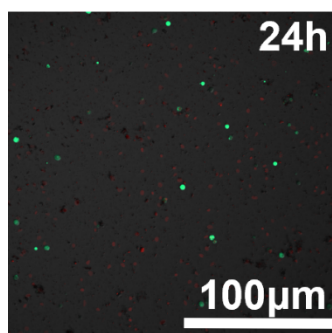


**Fig. S12.** GL261 cells were inhibited within 24 h by the UCNPs@mSiO<sub>2</sub>-Dox@TA-Al (100 µg/mL) nanoparticles in calcein-acetoxymethyl (AM)/propidium iodide (PI) co-staining.

References:

1. Liu, B.; Sun, J.; Zhu, J.; Li, B.; Ma, C.; Gu, X.; Liu, K.; Zhang, H.; Wang, F.; Su, J.; et al. Injectable and NIR-Responsive DNA-Inorganic Hybrid Hydrogels with Outstanding Photothermal Therapy. *Adv Mater* **2020**, *32*, e2004460, doi:10.1002/adma.202004460.